New Control Strategy for the Weekly Scheduling of Insular Power Systems with a Battery Energy Storage System

G.J. Osório[a], E.M.G. Rodrigues[a], J.M. Lujano-Rojas[a,b,c], J.C.O. Matias[a], J.P.S. Catalão[a,b,c*]

[a] *University of Beira Interior, R. Fonte do Lameiro, Covilha, Portugal*
[b] *INESC-ID, R. Alves Redol, Lisbon, Portugal*
[c] *IST, University of Lisbon, Av. Rovisco Pais, Lisbon, Portugal*

Received 6 September 2014

Abstract

The increment in generation costs is one of the most important factors that characterizes the operation of insular power systems, and is related to the location of these systems and the type of fuel used to provide electricity. This situation motivates the integration of renewable generation at high rates, as well as energy storage systems (ESSs), to improve the utilization of these resources. In this paper, a new control strategy is presented for the day-ahead scheduling of insular power systems with a battery energy storage system. The method presented here incorporates the effects of the most relevant components such as thermal generators, wind power generation, power converter, charge controller and ESS, being integrated into the scheduling process of insular power systems as a new contribution to earlier studies. The results provided show a fuel saving of 2% and an improvement in the wind power use of 20%, which is significant.

Keywords: Battery energy storage system; Economic dispatch; Insular power systems; Renewables integration; Unit commitment; Vanadium redox battery.

1. Introduction

High generation costs are possibly the most significant characteristic of insular power systems, owing to their isolated locations; a factor that makes their connection to other mainland power systems either difficult or impossible, and which increases the costs related to the transportation of the required fuels, which, in many cases, are heavy fuel oil (HFO) and light fuel oil (LFO). This situation has motivated the development and implementation of renewable power sources, such as wind energy and photovoltaics (PV) energy [1-4]. The exploitation of renewable resources is related to the geographical location so that those systems located near to the equator will develop solar energy; some examples are the Canary Islands, Cyprus, and Hawaii.

In contrast, islands located far from the equator will develop other renewable sources, such as biomass or hydropower; for instance, Samsoe (Denmark) and New Zealand. People's knowledge and involvement has been recognized as a key factor in the successful deployment of renewable energy on islands. Nevertheless, the main obstacle is related to the legislation and administrative barriers.

This context has meant that on some islands grid-parity with PV generation has been reached. An example is the case of Cyprus, where, according to the study carried out by Fokaides and Kylili [5], the high electricity prices make the power generation from PV panels profitable.

A high penetration of renewable sources can introduce problems for the optimal management of this type of system, owing to the fact that these sources have a stochastic nature that introduces uncertainty into the scheduling process. To deal with this problem, the incorporation of stochastic relations in the unit commitment formulation (UC), the integration of energy storage systems (ESSs), and demand response programs (DRs) have been suggested in the literature.

Battery energy storage systems (BESSs) have had special attention for several years. From a global perspective, the potential for the installation of BESSs in isolated power systems is estimated at 5300 MWh. The incorporation of BESSs can reduce the levelized cost of energy (LCOE) by 6%, and increase the penetration of renewable energies by approximately 50% to 70%.

*Corresponding author at: University of Beira Interior, R. Fonte do Lameiro, 6201-001 Covilha, Portugal. Tel.: +351 275 329914; fax: +351 275 329972. *E-mail address*: catalao@ubi.pt (J.P.S. Catalão).

In the case of regions with high-class solar resources, BESSs improve the correlation between solar radiation and load profile, and allows using the power generated during the day to supply peak demand, which usually occurs during the evening. However, the integration of BESSs with wind energy could be affected negatively by the variability of this resource, as there could be long time periods without any wind generation. This lack of wind power requires an increment in the size of BESSs, which increases the cost of the project [6]. Pumped hydro energy storage (PHES) has become a popular method for improving the flexibility of the power system. Recently, the installation of PHES, to be operated jointly with a wind farm, has been proposed to supply energy demand in Karpathos and Kasos, (Greece). To manage PHES, the water required to be stored in the upper reservoir will be supplied by wind generation whenever it is available, and by thermal generators during the night, when energy demand is low and a shortage of stored water occurs [7].

A representative example of incorporation of PHES to insular power systems is the case of Ikaria Island (Greece). This system is composed by 15.85 MW of diesel generation, wind generation with a total capacity of 1835 MW, a PV system with total capacity of 1040 kW, and 3 water reservoirs. For the optimal management of PHES, Papaefthymiou et al. [8] have developed an algorithm that consists of six main steps: in the first step, it requests the independent system operator (ISO) the power and energy necessities for the next day, which should be supplied by PHES. In the second step, PHES presents the corresponding energy offer determined through wind power forecasting. During the third step, PHES presents a declaration of load that is required to supply the energy demand of ISO, which is carried out when energy required by ISO is higher than the expected energy production of PHES. In step four, ISO dispatches the power from/to PHES. In step five, ISO dispatches thermal generators. Finally, in step six, power from external wind farms is determined and dispatched.

It has been suggested that PHES technology be integrated into the power system of Lesvos, where a detailed economic analysis has been carried out in [9], concluding that from the perspective of an investor, the optimum size is sensitive to the applicable energy and capacity tariffs, as well as wind potential and capital cost. Moreover, from the perspective of the power system, in those systems powered by HFO, LCOE could be reduced and renewable power penetration could be increased, by integrating a small-capacity PHES. On the other hand, when the system is powered by LFO, a PHES of larger capacity is required since the power generation from renewable sources is increased.

Nowadays, the management and optimal control of EESs is an important topic that has been widely analyzed in the technical literature, with several approaches proposed. Senjyu et al. [10] developed a methodology for the scheduling of power systems with thermal generators and an ESS. In this approach, an ESS is used to reduce the peak load and total generation cost. The scheduling process is carried out in three steps: in the first step, the scheduling of thermal units is done by applying an enhanced priority list (EPL) method, in order to reduce the computational time; in the second and third steps, an algorithm is applied to incorporate the ESS into the scheduling process. A BESS is modelled by using linear expressions for charging and discharging processes, while the inverter has an ideal behaviour. The charge of the BESS is done by using the excess of electricity from the committed generators. However, if this is not enough, more units could be committed, in order to charge the batteries up to a determined state of charge level. The discharge is done during the peak load, in order to avoid the necessity of using the most expensive generators, which can be shut down for short time intervals. After the analysis of several study cases, the results have shown a reduction in the generation costs of between 1.1% and 1.5%.

Mohammadi and Mohammadi [11] developed an optimization methodology to design ESS to be integrated into microgrids. The developed method is based on the solution to the stochastic UC problem, using the scenario-generation/reduction method in order to consider the different sources of uncertainty in a horizon-schedule of 24 h, with a step of 15 min. The optimization is formulated as a mixed-integer problem, and is solved by using an improved version of the Cuckoo Optimization Algorithm. This problem is subject to several constraints related to the energy balance of the electrical and thermal loads, the operation of the boiler, battery, and the power grid. Several technologies for the ESS are considered, such as hydrogen, thermal and BESS. Three management strategies are analyzed: two of them to design and manage BESS; and another to manage the thermal energy storage. The effects of incorporating ESS into the microgrid were analyzed in several case studies, obtaining a reduction in generation costs.

Chen et al. [12] proposed a model to design an ESS to be integrated into a microgrid. The methodology is based on determining the peak-shaving and excess of electricity according to the operating conditions, in order to determine the minimum energy to be supplied by the storage system, and to be charged into it. In addition, two mathematical models are proposed: one to the islanded system; and the other to the grid-connected systems. For the islanded microgrid, the UC problem incorporating renewable generation and ESS is solved, while for the grid-connected system, the economic benefits are considered to be the objective of the optimization process.

Daneshi et al. [13] presented a methodology to control a compressed air energy storage system (CAES) in order to provide ancillary services. The proposed method is based on the solution of the security constrained UC problem. The effects of the integration of CAES on locational pricing, peak-load shaving, power flows on the transmission grid, wind curtailment, and emissions are analyzed.

Nazari et al. [14] proposed a method that incorporates PHES in the UC of thermal generators, taking into account environmental constraints. The methodology presented in this paper consists of two stages: in the first stage, the scheduling of PHES is determined, in order to modify the shape of the load profile, to improve the operation of the thermal units; in the second stage, the scheduling of thermal generators is determined, considering the changes introduced by PHES in the first stage. Results obtained from the analysis of a case study have revealed a reduction of 1.2% in the generation cost.

Ming et al. [15] proposed a methodology for the integration of wind power and PHES in the UC problem, using a Binary Particle Swarm Optimization (BPSO) algorithm with several adjustments, in order to achieve a feasible solution. These adjustments are related to the minimum up/down time constraint, limits on the power generation and ramp constraints, power balance, and PHES operation. The economic benefits of the implementation of PHES are observed in the reduction of the peak load.

Jiang et al. [16] developed a model based on a robust optimization approach whereby the random variables are set, taking into account the worst situation, instead of establishing assumptions based on the probability distributions. The model is formulated as a two-stage robust optimization problem, where wind power production is assumed to be within a determined interval that could be obtained by using quantiles. Moreover, the conservatism of the obtained solution is controlled by introducing an integer variable that represents the number of hours that are allowed for sudden changes in the wind power production. The incorporation of PHES allows the reduction of the generating costs, while the robust optimization guarantees a reliable solution owing to the consideration of the worst-case scenario.

Khodayar et al. [17] proposed an optimization model for integration between wind power generation and PHES, in order to reduce variability, and improve its ability to be dispatched. This approach is based on the solution of the stochastic security constrained UC problem, through the scenario-generation approach, in order to incorporate several sources of uncertainty, such as forecasting error of load demand and wind generation, besides system reliability. The optimization is formulated as a mixed-integer programming problem, which is solved by using Benders' decomposition technique.

Suazo-Martinez et al. [18] developed an optimization model to integrate ESSs into the electricity market. The optimization model uses a two-stage stochastic UC formulation that aims to maximize the economic benefits; specifically, the integration of ESS is evaluated for providing primary reserve, energy arbitrage, and secondary reserve, considering different storage capacities. According to the results obtained from the analysis of a case study, the incorporation of an ESS reduces the participation of expensive generation units, such as those based on diesel and fuel-oil in the power balance, and allows the supply of the secondary reserve in a cheap manner, using energy generated from those units with low operating costs, such as coal units. When an ESS is used for energy arbitrage, the operating efficiency of the system is improved, and the generation costs are reduced by approximately 0.5%, Moreover, when an ESS is used for energy arbitrage and secondary reserve, generation costs are reduced by approximately 1.1%. In brief, using ESSs to provide different services improves the accommodation of renewable energies; it reduces the participation of the most expensive generators in the power balance, and reduces the operating costs of the power system.

Yu et al. [19] introduced a model to find the optimal size and location of an ESS, to improve the operation of distribution systems by reducing the risk related to the electricity price volatility, and the maximization of the economic profit. In this approach, the size of the ESS depends on the forecasting error of the load demand, and the power production of the distributed sources. This characteristic allows a reduction in the required capacity of the storage system, which consequently improves the economic performance of the project. Moreover, information about power exchange between the substation and the grid is used to optimize power purchasing, in order to maximize the benefits, and improve power flow through the distribution system. This optimization problem is solved by using a fuzzy particle swarm optimization algorithm.

Pozo et al. [20] presented a model of an ESS for the general purpose of mitigating the effects of variability and the uncertainty of renewable generation in the power system. The main advantage of the proposed model is that it can be incorporated in regular deterministic and stochastic mixed-integer optimization formulations, which are frequently implemented in large-scale systems. A sensitivity analysis of the most important parameters of the storage system, such as the storage and power production efficiencies and costs, was carried out. The obtained results showed how the operating costs increase as the storage costs increase. Moreover, the generating costs decrease as efficiency increases.

In this paper, a new control strategy to be used in the weekly scheduling of insular power systems with BESSs is presented. The methodology described here incorporates the effects of the most relevant components such as thermal generators, wind power generation, power converter, charge controller and BESS. As can be noted from the literature review described previously, the joint effect of these elements in the scheduling process of insular power systems has not been considered, so the development of new control strategies incorporating this feature is of the utmost importance. The proposed method consists of two major steps. In the first step the UC problem is solved without taking into account BESS; from this procedure the total energy available to charge BESS is estimated. While in the second step, using the estimated energy available obtained in the first step, the BESS is incorporated to the UC problem.

The rest of the paper is organized as follow: Section 2 describes the architecture of the power system under analysis, the mathematical models of the thermal and renewable generators, power converter, BESS and charge controller. In Section 3, the proposed methodology is explained. In Section 4, the proposed method is illustrated through the analysis of a case study, while final conclusions are presented in Section 5.

2. Power System under Analysis

The structure of the insular power system with the BESS to be analyzed is presented in Fig. 1. The system consists of several thermal generators that could be steam turbines, combined-cycle gas turbines, diesel engines, and open-cycle gas turbines. As was stated before, these units could be powered by HFO and LFO. Another important component of this type of system is the renewable generation, which in our case is considered to be obtained from the wind. The BESS is composed of the power converter, the charge controller, and the storage system, which in our case was assumed to be a Vanadium Redox battery (VRB). VRB technology was selected for illustrative purposes; since the proposed methodology has a flexible feature, other technologies such as lead-acid batteries with non-linear behavior could be easily integrated. A VRB allows the storage of the excess of electricity generated by thermal and renewable units. A charge controller guarantees the correct use of the VRB, to prevent its overcharging or undercharging, and the power converter carried out the DC-to-AC conversion, and vice versa. Under a high penetration of renewable sources, it is possible to produce an excess of electricity that could not be stored in a VRB. Then, in order to preserve system stability, this excess of energy has to be consumed by the dump load.

"Figure 1"

In the next subsections, each element of the insular power system is going to be described in a detailed manner.

2.1. Thermal and Renewable Generation Units

In the framework of UC problem, thermal generation units are modelled through their fuel consumption estimation, starting-up cost, power generation limits, startup and shutdown ramp rates, operating ramp rates, and minimum up/down time constraints. Typically, fuel consumption is modelled by using the quadratic expression of equation (1),

$$f_i^t = a_i + b_i P_i^t + c_i (P_i^t)^2 \tag{1}$$

where a_i, b_i and c_i are parameters related to the fuel consumption of the unit *i*, f_i^t is the fuel consumption of generator *i*, and P_i^t is the power generation of unit *i* at time *t* (*i* = 1, 2, …, *N* and *t* = 1, 2, …, *T*). The cost related to the starting-up of a determined generator could be modelled by using the simplified expression of equation (2),

$$SUC_i^t = \begin{cases} HSU_i;\ T_{off,i}^t \le MDT_i + CST_i \\ CSU_i;\ T_{off,i}^t > MDT_i + CST_i \end{cases} \tag{2}$$

where SUC_i^t is starting-up cost, HSU_i^t is the hot startup cost, CSU_i^t is the cold startup cost, CST_i is the cold startup time of unit *i* at time *t*. The variables $T_{on,i}^t$ and $T_{off,i}^t$ are calculated by means of equations (3) and (4).

$$T_{on,i}^t = \begin{cases} T_{on,i}^t + 1;\ U_i^t = 1 \\ 0;\qquad\qquad U_i^t = 0 \end{cases} \tag{3}$$

$$T_{off,i}^t = \begin{cases} T_{off,i}^t + 1;\ U_i^t = 0 \\ 0;\qquad\qquad U_i^t = 1 \end{cases} \tag{4}$$

where $T_{on,i}^t$ is the cumulative number of hours until the present instant (*t*) that generator *i* has been online, similarly $T_{off,i}^t$ is the cumulative number of hours until the present instant (*t*) that generator *i* has been offline. MUT_i and MDT_i are minimum up time and minimum down time of unit *i*, respectively. U_i^t is the status of unit *i* at time *t*, where 0 represents de-committing, while 1 represents the committing of respective generation unit. In each time step, power production of a determined unit is constrained by the maximum and minimum capacity of the unit and its corresponding ramp constraint. This is mathematically expressed through equations (5)-(7).

$$P_i^{min} \leq P_i^t \leq P_i^{max};\ U_i^t = 1 \tag{5}$$

$$P_i^t - P_i^{t-1} \leq UR_i;\ U_i^t = 1\ \ U_i^{t-1} = 1 \tag{6}$$

$$P_i^{t-1} - P_i^t \leq DR_i;\ U_i^t = 1\ \ U_i^{t-1} = 1 \tag{7}$$

where P_i^{min}, and P_i^{max} are the minimum and maximum power production of unit i, respectively. Meanwhile, UR_i and DR_i are ramp up and down of unit *i*, respectively. The ramp constraints during starting-up and shutting down of determined generators are represented by using the constraints of equations (8) and (9),

$$P_i^t \leq SUR_i;\ U_i^t = 1\ U_i^{t-1} = 0 \tag{8}$$

$$P_i^t \leq SDR_i;\ U_i^t = 1\ U_i^{t+1} = 0 \tag{9}$$

where SUR_i and SDR_i are startup ramp and shutdown ramp of unit *i*, respectively. Typically, thermal units have to be online or offline during a determined time length, this restriction is incorporated by using the equations (10) and (11),

$$T_{on,i}^t \geq MUT_i \tag{10}$$

$$T_{off,i}^t \geq MDT_i. \tag{11}$$

Wind power generation is modelled as controllable source, where the maximum capacity is defined by the available wind power obtained from the forecasting process. This idea is expressed in equation (12),

$$0 \leq W^t \leq W_{max}^t \tag{12}$$

where W^t is the wind power production determined from the optimization process and W_{max}^t is the forecasted wind power production.

2.2. Power Converter

The connection between the ESS and the power grid of the insular system is carried out using electronic power converters. The technology of this connection device can be divided into three different categories: standard, multilevel, and multiport topologies. Standard topology is divided into single-stage and double-stage. Single-stage is the simplest topology that consists of a bidirectional DC/AC converter, while double-stage consists of a DC/DC stage and a DC/AC stage. The DC/DC stage adjusts the DC voltage to a reasonable level, so that DC/AC stage can be connected directly to the distribution system.

Multilevel topology allows the obtaining of the required AC voltage from several levels of DC voltages. On the other hand, multiport topology is provided with a single-stage with multiple ports, which can interface the ESS with the grid in a reduced number of stages, improving the efficiency with a reduced cost and a simple control strategy [21].

In a general sense, the efficiency of the DC-to-AC conversion process depends on the load to be supplied, DC voltage, and temperature [22]. The simplified model used in this paper estimates the efficiency of the power converter by means of equation (13) [23],

$$\eta_v = \frac{P_v}{m_0 P_v^{rated} + (1 + m_1) P_v} \tag{13}$$

where η_v is the efficiency of the power converter, P_v^{rated} is the rated power of the inverter and P_v is the power through the inverter. m_0 and m_1 are parameters to be determined by using experimental information, the values assumed here are m_0 = 0.0119 and m_1 = 0.0155.

2.3. VRB and Charge Controller Model

In VRB storage technology, energy and power are independents each other, giving more flexibility to improve power system operation. The rated power is determined by the capacity of the VRB stack, while the total energy to be stored is determined by the amount of electrolyte. Besides of this, state-of-charge (SOC) can be determined with precision by means of the amount of electrolyte remaining. Other important feature is its fast response due to the speed of the chemical reaction [24, 25].

In general sense, VRB is important to improve the operation of isolated system as well as grid-connected systems with high penetration of renewable power sources [26]. In this paper, SOC of VRB is estimated by using equation (14),

$$SOC_t = SOC_{t-1} + \frac{P_{bt}^t \Delta t}{E_{max}} \eta_b F \quad (14)$$

where SOC_t is the state of charge of VRB at time t, P_{bt}^t is the power to charge or discharge VRB, positive to the charge and negative during discharge, E_{max} is the maximum energy to be stored on VRB, Δt is the time step of the simulation, η_b is the efficiency of VRB, and F is the control factor, this factor represents the actions carried out by the charge controller during the charge process. Mathematical definition of factor F is presented in equation (15),

$$F = \begin{cases} max\left(1 - e^{\left[\left(\frac{m_2}{\frac{P_{bt}^t}{P_{max}} + m_3}\right)(SOC_t - SOC_{max})\right]}, 0\right); & P_{bt}^t > 0 \\ 1; & P_{bt}^t < 0 \end{cases} \quad (15)$$

where P_{max} is the rated power of VRB stack, m_2 and m_3 are parameters to define how charge controller manage the charge process. In this paper, considering some experience from lead acid batteries these parameters were fixed to m_2 = 20.73 and m_3 = 0.55 [27]. SOC_{min} and SOC_{max} are the minimum and maximum SOC allowed to be reached by VRB. Typically, SOC_{max} = 0.9 according to the suggestions of the manufacturers. Equations (14) and (15) are expressed as single non-linear equation, which is solved by using Bisection method in order to determine SOC_t.

In order to illustrate the operation of the charge controller, the charging process of a VRB of 7 kW/40 kWh was simulated. SOC_{min} and SOC_{max} are assumed to be 0.2 and 0.9, respectively, while the charge and discharge efficiencies (η_b) were assumed to be 0.8. Charge process was simulated considering different initial SOC between 0.2 and 0.8. The results from the simulations are presented in Fig. 2. The proposed model described in equations (14) and (15) was used to estimate the power required from the grid to charge the VRB, considering the effects of the charge controller. It is possible to observe how the charge controller gradually reduces the power absorbed from the grid as the VRB reaches its maximum SOC. This explains the role of the term F introduced in equation (15).

"Figure 2"

3. UC Problem Incorporating BESS

As was stated before in the introduction section, the proposed approach consists of two main steps: in the first step, the excess of power generation and the curtailed wind power are estimated from the solution of the UC problem, without taking the BESS into account; then, in the second step, the management of the BESS is carried out considering the excess of energy generated and the curtailed wind power obtained from the first step. In the following subsections, the proposed approach and the methodology used to solve UC problem are described.

3.1. Proposed Approach

The proposed methodology in this paper aims to store the excess of power generated and the curtailed wind power during low load periods, in order for this excess of power stored to be discharged during high energy demand periods. The proposed methodology can be applied by implementing the algorithm presented as follow:

Step 1: Solve UC problem by priority list (PL) method without considering BESS, from the solution determine the excess of thermal power generation (ETG^t) for each time instant t. The term ETG^t is the excess of thermal power generation. This excess of energy is produced when load demand is lower than the minimum power generation of the committed units. Typically, this excess of energy is consumed by the dump load; however, it could be used for charging BESS.

Step 2: Determine the available charging power of BESS (CP^t), applying equation (16),

$$CP^t = ETG^t + (W_{max}^t - W^t) \quad (16)$$

Step 3: Create the binary vector of battery state according to the available charging power (BS_{WC}^t). In this vector, 1 means charging and 0 means discharging.

If there is power to charge, BESS (CP^t > 0); BS_{WC}^t = 1, in other case BS_{WC}^t = 0. In other words, if there is power available, BESS should be charged, in the contrary case, BESS should be discharged to minimize fuel consumption. Fig. 3 illustrates how to build this vector under different operating conditions.

"Figure 3"

Step 4: Create the vector of binary state according to the shape of the load profile (BS^t_{shape}). As is shown in Fig. 4, the state of BESS is determined taking into account the geometry of the profile. Let D_{avg} be the average value of the hourly load which is the mean value of the load profile over the entire horizon of forecasting; if $D^t < D_{avg}$, load should be increased, while in the contrary case, load should be reduced. This strategy makes the shape of the load profile uniform, while reduces the commitment of thermal units.

"Figure 4"

Step 5: Once vectors BS^t_{WC} and BS^t_{shape} have been built, the reference power of BESS (RP^t) is created. This vector is the power set point of BESS for a determine time instant *t*. For any value of *t*; if $BS^t_{shape} = 0$ and $BS^t_{WC} = 0$, $RP^t = W^t_{max} - D^t$, else $RP^t = CP^t$. In this step is guaranteed that BESS is discharged only in those time period so that the load profile becomes flattened. After this, the signal of reference to the BESS is completed. Positive elements of RP^t correspond to charge periods; while, negative elements correspond to discharge periods. The signal RP^t obtained is illustrated in Fig. 5.

"Figure 5"

Step 6: Using RP^t, the periods of charge and discharge are defined. In the case presented in Fig. 5, charge period corresponds to the hours between t_i and t_o, while discharge period corresponds to the hours between t_o and t_f. Considering the initial SOC ($SOC_{t=0}$); if the next period corresponds to a charging one, SOC at the end of this period is estimated by using the BESS model of Section 2. On the contrary, if the next period corresponds to discharge, the energy stored into BESS to be discharged (E_o) is estimated by using equation (17),

$$E_o = (SOC_t - SOC_{min})E_{max} \tag{17}$$

and the discharge power (P_d) is determined from equation (18),

$$\frac{E_o}{\eta_b} = \sum_{t=t_o}^{t=t_f} |\max(W^t - D^t, -P_d)|\Delta t \tag{18}$$

where variable P_d is limited between 0 and a determined value ($P^o_{d,max}$). In this step, the variable $P^o_{d,max}$ is assumed to be equal to P_{max} ($0 \le P_d \le P^o_{d,max}$). The value of the variable P_d is determined from equations (17) and (18) by means of Bisection method.

Step 7: Using the value of P_d obtained in Step 6, the behavior of BESS is estimated by evaluating the VRB model of Section 2. The power exchanged between BESS and the power system (see Fig. 2) obtained from VRB model is represented by the variable P^t_{BESS}. The power absorbed or supplied by VRB considering the effects of charge controller are saved in the variable P^t_{BESS} through the hourly cycle.

Step 8: When BESS is incorporated to the UC problem, it is assumed to be the unit with highest priority in the system, so that the power to be supplied by thermal units and wind generator (G^t) is assigned according to the equation (19),

$$G^t = D^t + P^t_{BESS} \tag{19}$$

where variable P^t_{BESS} has the same sign convention of the vector P^t_{bt}.

Step 9: Now, the UC problem is solved considering the time series (G^t) instead of D^t. The excess of thermal generation (ETG^t) is checked. If there is some excess of electricity, the maximum power to be discharged previously estimated in Step 6 ($P^o_{d,max}$) is limited to a new value ($P^f_{d,max}$) and calculated according to equation (20):

$$P^f_{d,max} = |P^o_{d,max}| - \max(ETG^t) \tag{20}$$

This reduction in the maximum discharging power allows us to reduce the excess of electricity. After this process, go to Step 6 assigning the value of $P^o_{d,max}$ with the value of $P^f_{d,max}$ previously calculated in equation (20). In other words, make the assignment $P^o_{d,max} \leftarrow P^f_{d,max}$.

On the contrary, if the excess of power generation is equal to zero and P_d is different of zero, the scheduling process has finished. However, if excess of electricity is higher than zero and $P_d \to 0$, this energy surplus will be absorbed by dump load DL^t.

3.2. Solving UC Problem by PL Method

The UC is an optimization problem that consists on minimize the total generation cost, which is expressed by means of the variable (z) in equations (21),

$$z = \sum_{t=1}^{T} \sum_{i=1}^{N} f_i^t + SUC_i^t (1 - U_i^t) U_i^t \tag{21}$$

This optimization problem is constrained to the general characteristics of thermal generators that have been described in equations (2)-(12) in Section 2. Other important constraints are related to the spinning reserve and power balance, which are presented in equations (22) and (23),

$$\sum_{i=1}^{i=N} P_i^{t,max} U_i^t - \sum_{i=1}^{i=N} P_i^t U_i^t \geq SR(D^t) + WFE(W^t) + BFE(P_{BESS}^t) \tag{22}$$

$$\sum_{i=1}^{i=N} P_i^t U_i^t + W^t + P_{bt}^t = D^t + DL^t \tag{23}$$

where $P_i^{t,max}$ is the maximum power production of unit *i* at time *t*, considering the ramp rate constraints. SR is the spinning reserve, WFE is the increment in spinning reserve due to wind power forecasting error, and BFE is the increment in spinning reserve due to the uncertainty in the power to be discharged from BESS.

As the BESS is charged from the curtailed wind generation which has uncertainty, the amount of power to be discharged during the periods of high load demand will have uncertainty. Hence, this uncertainty on the power to be discharged is compensated by means of the BFE term. The PL method offers a near-optimal solution to the UC problem in a reduced computational time. In particularly, in cases with a high integration of renewable sources, where the load to be supplied by thermal generators is low, the PL method can provide a reasonable solution, in contrast with other methodologies that have great difficulty in finding a feasible solution [28].

Recently, this method has evolved in an important manner. In [29] is proposed a methodology in which thermal generators are committed by following a probability distribution function. In [30] is proposed a method that combines an improved version of the PL method, and an augmented Hopfield Lagrange (AHL) neural network. In [31], an improved pre-prepared power demand (IPPD), in combination with the Muller method, was introduced. In [32] is proposed a combination based on an improved Lagrangian relaxation (ILR) and AHL.

The PL method consists of several steps that allow us to obtain a cost-effective and feasible solution to the UC problem. These steps are primary unit scheduling, minimum up/down time repair, spinning reserve repair, shutdown repair, unit substitution, and the shutdown of the power surplus. A brief description of these steps is described as follow.

3.2.1. Primary Unit Scheduling

In PL method, all generators are committed according to their average production cost (f_i^{avg}) that is defined by equations (24) and (25),

$$f_i^{avg} = \frac{a_i + b_i\left(P_i^{avg}\right) + c_i\left(P_i^{avg}\right)^2}{P_i^{avg}} \tag{24}$$

$$P_i^{avg} = \frac{P_i^{max}}{2}\left(1 + \frac{P_i^{min}}{P_i^{max}}\right) \tag{25}$$

where P_i^{avg} is the average power generation of unit *i*. An initial approximation to UC problem is obtained by following the next algorithm:

Step 1: Built the matrix to save the primary unit scheduling (PUS_i^t), this matrix has $N + 1$ rows and T columns; an additional row is added in order to consider the production of the wind generation. The values of all the elements in this matrix that corresponds to thermal generators are assumed to be zero.

Step 2: Establish the order at which the units will be committed, this is carried out using f_i^{avg} index presented in equation (24).

Step 3: Set $t \leftarrow 1$.

Step 4: According to the priority list of Step 2, the first generator of the list is chosen by setting $i \leftarrow 1$.

Step 5: Set $PUS_i^t \leftarrow 1$.

Step 6: Check the maximum capacity committed in Step 4 without considering the ramp constraints. If the spinning reserve constraint is not fulfilled and $i \leq N$; set $i \leftarrow i + 1$ and go to Step 5; else if $t \leq T$ set $t \leftarrow t + 1$ and go to Step 4; else stop.

3.2.2. Minimum Up/Down Time Repairing

The initial approximation obtained from the primary unit scheduling procedure described before does not satisfy the minimum up/down time constraint. For this reason, a repairing process has to be introduced. An example of the repairing process of minimum up time constraint is shown in Fig. 6, where the rows that correspond to the unit i of the matrices PUS_i^t and U_i^t are presented. In order to fulfill the condition $MUT = 5$ this unit is committed during for four additional hours.

"Figure 6"

Fig. 7 illustrates the methodology to repair those cases where minimum down time constraint is violated. In this case, generator i should be offline during at least three hours ($MDT = 3$) so that, in order to fulfil this constraint unit i is committed during two additional hours.

"Figure 7"

In [30] a complete algorithm to repair minimum up/down time constraint has been developed and it will be used in this paper. This will be briefly described next:

Step 1: Using the matrix PUS_i^t, estimate the cumulative number of hours that unit i has been online ($T_{on,i}^t$) and offline ($T_{off,i}^t$), using equations (3) and (4), respectively.

Step 2: Set $t \leftarrow 1$.

Step 3: Set $i \leftarrow 1$.

Step 4: If ($PUS_i^t = 0$) and ($PUS_i^{t-1} = 1$) and ($T_{on,i}^t < MUT_i$); set $U_i^t \leftarrow 1$.

Step 5: If ($PUS_i^t = 0$) and ($PUS_i^{t-1} = 1$) and ($t + MDT_n - 1 \leq T$) and ($T_{off,i}^{t+MDT_i-1} < MDT_i$); set $U_i^t \leftarrow 1$.

Step 6: If ($PUS_i^t = 0$) and ($PUS_i^{t-1} = 1$) and ($t + MDT_i - 1 > T$) and ($\sum_{k=t}^{T} PUS_i^k > 0$); set $U_i^t \leftarrow 1$.

Step 7: Estimate the matrices $T_{on,i}^t$ and $T_{off,i}^t$.

Step 8: If ($i < N$); set $i \leftarrow i + 1$ and go to Step 4.

Step 9: If ($t < T$); set $t \leftarrow t + 1$ and go to Step 3; else stop.

3.2.3. Spinning Reserve Repairing

The scheduling obtained from the primary unit scheduling and the repairing of minimum up/down time constraint could not fulfil the spinning reserve requirements due to the effects of the ramp rates of the different generators. To overcome this problem, more generation is added by the following algorithm:

Step 1: For $t = 1, 2, \ldots, T$, verify spinning reserve requirements using equation (22).

Step 2: Create a list with those hours at which spinning reserve requirements are not fulfilled. The number of elements of this list is represented by the variable B.

Step 3: If ($B > 0$); create a table with B rows and two columns. This table will save the generators and hours at which they should be committed in order to fulfil the spinning reserve requirements. In other case; stop.

Step 4: The list created in Step 2 is saved in the second column of the table created in Step 3.

Step 5: For each element of the list created in Step 2, identify the potential generators to be committed according to the priority list. These generators are saved in the first column of the table created in Step 3.

Step 6: The first two elements (first element of column one and two) of the table previously filled are selected. Then, the condition of the corresponding unit is changed from offline to online.

Step 7: As the condition of this unit has changed, the repairing of minimum up/down time constraint is carried out in order to fulfil these constraints.

Step 8: Go to Step 1.

3.2.4. Shutdown Repairing

At this stage, it is likely that some generators could not be shut down because of the violation of the respective condition. To solve this problem, it is necessary gives more time of operation to these units so that they can be lead offline. The repairing process used in this paper is explained as follow:

Step 1: For $t = 1, 2, \ldots, T$, verify the violation of shutdown ramp constraint using equation (9).

Step 2: Create a list with those generators at which shutdown ramp constraint is violated and the corresponding hours that should be additionally committed in order to fulfil this constraint. This list is saved in a table whose first column represents the units and second column represents the additional hours that they should be committed.

Step 3: If the list is not empty, the first two elements (first element of column one and two) of the table previously filled are selected. Then, the condition of the corresponding unit is changed from offline to online. On the contrary, stop.

Step 4: As the condition of this unit has changed, the repairing of minimum up/down time constraint is carried out in order to fulfil these constraints.

Step 5: Go to Step 1.

3.2.5. Unit Substitution

During in peak hours, some units are committed during more hours than those required in order to fulfil minimum up time constraint. This situation could be easily understood by analysing Fig. 6, where the corresponding unit has been committed during four additional hours to fulfil minimum up time constraint. However, a cheaper scheduling could be obtained by using another unit with minimum up time of one hour.

In order to identify those generators to be substituted, the matrix CH_i^t of the changes in the primary unit scheduling due to the repairing of minimum up/down time constraint is created. CH_i^t is calculated from the subtraction between U_i^t and PUS_i^t. Another matrix (S_i^t) is built in order to store the units and the corresponding hours at which they are going to be substituted, this matrix has a similar structure to the matrix U_i^t in the sense that both of them are binaries. If a determined unit *i* will be substituted at the time *t*, $S_i^t = 1$; on the other hand, if this generators is not going to be substituted, $S_i^t = 0$.

An extended analysis of a unit with $MUT_i = 3$ is presented in Fig. 8, the rows of the matrices PUS_i^t, U_i^t, CH_i^t, $T_{on,i}^t$, and S_i^t in the time interval between $t = 1$ and $t = 7$ are presented. It is possible observe that in $t = 3$, matrix $CH_i^3 = 0$, this allows to recognize any change in the scheduling. Moreover, $T_{on,i}^3 = 1$ and $T_{on,i}^6 = 0$, these values are obtained because unit *i* is committed during its minimum up time. Other important point is that $\sum_t^6 CH_i^t = 2$ which is higher than 0, this reflects the number of changes in the scheduling. The elements of S_i^t between $t = 3$ and $t = 5$ are equal to 1.

"Figure 8"

This illustrative example allows us developing an algorithm to know the generators to be substituted and the corresponding hours, this algorithm is presented next:

Step 1: Calculate the matrix CH_i^t as the subtraction between U_i^t and PUS_i^t.

Step 2: Initialize the matrix S_i^t to zero.

Step 3: Set $n \leftarrow 1$.

Step 4: Set $t \leftarrow 1$.

Step 5: If ($CH_i^t = 0$) and ($T_{on,i}^t = 1$) and ($t + MUT_i < T$) and ($T_{on,i}^{t+MUT_i} = 0$) and ($MUT_i > 1$) and ($\sum_t^{t+MUT_i-1} CH_i^t > 0$), the elements of S_i^t from t to $t + MUT_i - 1$ are assigned to 1; else if ($CH_i^t = 0$) and ($T_{on,i}^t = 1$) and ($t + MUT_i - 1 = T$) and ($T_{on,i}^{t+MUT_i-1} = MUT_i$) and ($MUT_i > 1$) and ($\sum_t^{t+MUT_i-1} CH_i^t > 0$), the elements of S_i^t from t to $t + MUT_i - 1$ are assigned to 1; else go to Step 6.

Step 6: If ($t < T$), set $t \leftarrow t + 1$ and go to Step 5; else go to Step 7.

Step 7: If ($i < N$), set $i \leftarrow i + 1$ and go to Step 4, else stop.

From the matrix S_i^t, the units that could be substituted are recognized. Then, all procedures described before are repeated; however, if the unit substitution process leads to a more expensive scheduling, the process is stopped.

3.2.6. Shutdown Excess of Committed Capacity

As can be observed in Figures (6) and (7), the repairing of minimum up/down time constraints produce an excess of spinning reserve which increments the total operation cost. In this procedure, this excess of committed capacity is found and shutdown to reduce operating costs. This is carried out by applying the algorithm described next:

Step 1: For $t = 1, 2, \ldots, T$, verify the excess of spinning reserve using equation (22).

Step 2: Create a list with those hours with excess of spinning reserve. The number of elements of this list is represented by the variable *J*.

Step 3: Set $m \leftarrow 1$.

Step 4: Considering the element *m* in the list created in Step 2, the most expensive generator is recognized and chosen as a candidate to be de-committed. If $T_{on,i}^t$ is higher than MUT_i, the generator *i* is de-committed.

Step 5: As a consequence of the Step 4, the unit scheduling is changed so that minimum up/down time constraint is repaired.

Step 6: Considering the scheduling obtained from Step 5, start/shutdown ramp constraints and spinning reserve are verified through equations (9) and (22), respectively. If at least one constraint is violated, the condition of the corresponding element is changed from 0 to 1.

Step 7: If ($m < J$), set $m \leftarrow m + 1$ and go to Step 4; else stop.

4. Case Study

The proposed strategy for the management of a BESS is illustrated by analysing a small-capacity insular power system of 5 diesel units, whose characteristics are presented in Table 1. These characteristics were obtained by using information provided by the manufacturers, although other costs, such as starting-up costs, have not been considered. Moreover, start-up and shutdown ramp rates and operating ramp rates have not been taken into account. Furthermore, it is assumed that these generators can deal with sudden changes in the load to be supplied. For all generators, minimum up/down times was assumed to be equal to 1 h.

"Table 1"

The time horizon of the scheduling process is 168 h (T = 168 h) that corresponds to one week. The wind power forecasted is presented in Fig. 9, while a forecasting error of 15% was assumed. The spinning reserve requirements were assumed to be 10% (SR = 0.1). The BESS is composed of a power inverter of 2000kW, and a VRB of 2000 kW/8000 kWh. The charge controller is settled to maintain SOC between 15% and 90% (SOC_{min} = 0.15 and SOC_{max} = 0.9), and the efficiency of VRB was assumed to be equal to 80% during charge and discharge processes (η_b = 0.8). The initial SOC of the VRB was assumed 15%. The increment in the spinning reserve, as a result of the wind power forecasting error (WFE) and uncertainty in the power obtained from BESS (BFE) was assumed to be equal to the forecasting error.

"Figure 9"

Fig. 10 shows the power interchange (P_{BESS}^t) between the BESS and the insular power system, while Fig. 11 shows the SOC of the VRB. On the one hand, it is possible to observe how the power available from the curtailed wind power is used to charge the VRB, and how the charge controller limits the SOC to 90% by reducing the charge power, specifically between t = 147 h and t = 165 h. On the other hand, it is possible to see how the proposed strategy controls the discharging process by adjusting the discharging power to a fixed value. Something relevant happens between t = 77 h and t = 143 h, where the VRB is discharged. However, the power interchanged with the system is almost zero ($P_{BESS}^t \rightarrow 0$), and this loss of power is a result of the low efficiency of the power inverter at this load.

"Figure 10"

"Figure 11"

Fig. 12 shows the load to be supplied by the thermal units and the wind generator when the BESS is incorporated. It is possible to see how the controlled discharge of the VRB by means of a uniform discharging power reduces the energy demand, particularly during the second and third days of our scheduling.

"Figure 12"

Tables 2 and 3 show the power production of the thermal units and the wind generators during day 2. In these tables it is possible to see how the incorporation of BESS reduces the power to be supplied by the thermal units, while it improves the accommodation of the wind power generation. Those generators removed from the scheduling owing to the operation of the BESS are presented in bold.

"Table 2"

"Table 3"

Over the scheduling horizon, fuel consumption without incorporating the BESS is 115755.80 liters, while the incorporation of the BESS reduces this value to 113784.30 liters, which represents a fuel saving of 1971.50 litres, about 2%.

Moreover, curtailed wind power without incorporating the BESS is 99620.70 kWh, while the after integration of the BESS, wind power curtailment is reduced to 79340.90 kWh. This represents an improvement in the wind power use of about 20%, which is significant.

Fig. 13 shows the analysis of BESS between t = 1 and t = 32, where on the left hand side it is shown the comparison between the available power to be stored on BESS, while on the right hand side, SOC of BESS is presented. From the analysis of the available energy comparison, an important difference between the available and stored energy can be seen; especially at t = 29, where the available power is 3939 kW, while stored power is 1530 kW. At this moment, $SOC_{t=29}$ = 0.704 is near to the established limit of 0.9; this behavior is highly influenced by the operation of the charge controller. In general sense, the amount of power to be curtailed from renewable resources have been reduced; however, not all the amount of power dispatched from renewable sources is effectively stored on BESS due to its operational limitations such as minimum and maximum SOC, and the charge controller operation, which leads to a limited reduction on fuel consumption of thermal generators.

"Figure 13"

The proposed approach was implemented in MATLAB programming language, using a standard PC with an i7-3630QM CPU at 2.40 GHz, 8 GB of RAM and 64-bit operating system. The computational time required to carry out this scheduling was only about 4 minutes.

5. Conclusions

In this paper, a new control strategy to be used in the weekly scheduling of insular power systems with BESSs was presented. The methodology proposed incorporated the effects of the most relevant elements such as thermal generators, wind power generation, power converter, charge controller and VRB. The proposed method consisted of two major steps: in the first step, the UC problem is solved without taking into account the BESS, and from this procedure the total energy available to charge the BESS is estimated; in the second step, using the estimated energy available obtained in the first step, the BESS is incorporated into the UC problem. The effectiveness of the proposed approach was illustrated by means of the scheduling of a 5-units system during one week. In comparison with the case without a BESS, a fuel saving of 2% could be reached from the integration of the BESS, while the accommodation of wind power generation could be improved by 20%, which was significant, for a CPU time of only 4 minutes.

Acknowledgements

This work was supported by FEDER funds (European Union) through COMPETE and by Portuguese funds through FCT, under Projects FCOMP-01-0124-FEDER-020282 (PTDC/EEA-EEL/118519/2010) and UID/CEC/50021/2013. Also, the research leading to these results has received funding from the EU Seventh Framework Programme FP7/2007-2013 under grant agreement no. 309048.

References

[1] Chua KJ, Yang WM, Er SS, Ho CA. Sustainable energy systems for a remote island community. Applied Energy 2014; 113: 1752-1763.

[2] Kapsali M, Anagnostopoulos JS, Kaldellis JK. Wind powered pumped-hydro storage systems for remote islands: A complete sensitivity analysis based on economic perspectives. Applied Energy 2012; 99: 430-444.

[3] Suomalainen K, Silva C, Ferrão P, Connors S. Wind power design in isolated energy systems: Impacts of daily wind patterns. Applied Energy 2013; 101: 533-540.

[4] Tao Ma, Hongxing Yang, Lin Lu, Jinqing Peng. Pumped storage-based standalone photovoltaic power generation system: Modeling and techno-economic optimization. Applied Energy 2014.

[5] Fokaides PA, Hylili A. Towards grid parity in insular energy systems: The case of photovoltaics (PV) in Cyprus. Energy Policy 2014; 65: 223-228.

[6] Blechinger P, Seguin R, Cader C, Bertheau P, Breyer Ch. Assessment of the global potential for renewable energy storage systems on small islands. Energy Procedia 2014; 46: 294-300.

[7] Katsaprakakis DA, Christakis DG, Pavlopoylos K, Stamataki S, Dimitrelou I, Stefanakis I, Spanos P. Introduction of a wind powered pumped storage system in the isolated insular power system of Karpathos-Kasos. Applied Energy 2012; 97: 38-48.

[8] Papaefthymiou SV, Karamanou EG, Papathanassiou SA, Papadopoulos MP. A wind-hydro-pumped storage station leading to high RES penetration in the autonomous island system of Ikaria. IEEE Transactions on Sustainable Energy 2010; 1(3): 163-172.

[9] Papaefthymiou SV, Papathanassiou SA. Optimum sizing of wind-pumped-storage hybrid power stations in island systems. Renewable Energy 2014; 64: 187-196.

[10] Senjyu T, Miyagi T, Yousuf SA, Urasaki N, Funabashi T. A technique for unit commitment with energy storage system. International Journal of Electrical Power and Energy Systems 2007; 29: 91-98.

[11] Mohammadi S, Mohammadi A. Stochastic scenario-based model and investigating size of battery energy storage and thermal energy storage for micro-grid. International Journal of Electrical Power and Energy Systems 2014; 61: 531-546.

[12] Chen SX, Gooi HB, Wang MQ. Sizing of energy storage for microgrids. IEEE Transactions on Smart Grid 2012; 3: 142-151.

[13] Daneshi H, Srivastava AK. Security-constrained unit commitment with wind generation and compressed air energy storage. IET Generation, Transmission & Distribution 2012; 6: 167-175.

[14] Nazari ME, Ardehali MM, Jafari S. Pumped-storage unit commitment with considerations for energy demand, economics, and environmental constraints. Energy 2010; 35: 4092-4101.

[15] Ming Z, Kun Z, Liang W. Study on unit commitment problem considering wind power and pumped hydro energy storage. International Journal of Electrical Power and Energy Systems 2014; 63: 91-96.

[16] Jiang R, Wang J, Guan Y. Robust unit commitment with wind power and pumped storage hydro. IEEE Transactions on Power Systems 2012; 27: 800-810.

[17] Khodayar ME, Shahidehpour M, Lei W. Enhancing the dispatchability of variable wind generation by coordination with pumped-storage hydro units in stochastic power systems. IEEE Transactions on Power Systems 2013; 28: 2808-2818.

[18] Suazo-Martinez C, Pereira-Bonvallet E, Palma-Behnke R, Xiao-Ping Z. Impacts of energy storage on short term operation planning under centralized spot markets. IEEE Transactions on Smart Grid 2014; 5: 1110-1118.

[19] Yu Z, Zhao YD, Feng JL, Ke M, Jing Q, Kit PW. Optimal allocation of energy storage system for risk mitigation of DISCOs with high renewable penetrations. IEEE Transactions on Power Systems 2014; 29: 212-220.

[20] Pozo D, Contreras J, Sauma EE. Unit commitment with ideal and generic energy storage units. IEEE Transactions on Power Systems 2014; 29(6): 2974-2984.

[21] Pires VF, Romero-Cadaval E, Vinnikov D, Roasto I, Martins JF. Power converter interfaces for electrochemical energy storage systems - A review. Energy Conversion and Management 2014; 86: 453-475.

[22] Rampinelli GA, Krenzinger A, Romero FC. Mathematical models for efficiency of inverters used in grid connected photovoltaic systems. Renewable and Sustainable Energy Reviews 2014; 34: 578-587.

[23] Lujano-Rojas JM, Monteiro C, Dufo-López R, Bernal-Agustín JL. Optimum load management strategy for wind/diesel/battery hybrid power systems. Renewable Energy 2012; 44: 288-295.

[24] Qiu X, Nguyen TA, Guggenberger JD, Crow ML, Elmore AC. A field validated model of a vanadium redox flow battery for microgrids. IEEE Transactions on Smart Grid 2014; 5: 1592-1601.

[25] Turker B, Klein SA, Hammer E-M, Lenz B, Komsiyska L. Modeling a vanadium redox flow battery system for large scale applications. Energy Conversion and Management 2013; 66: 26-32.

[26] Schreiber M, Harrer M, Whitehead A, Bucsich H, Dragschitz M, Seifert E, Tymciw P. Practical and commercial issues in the design and manufacture of vanadium flow batteries. Journal of Power Sources 2012; 206: 483-489.

[27] Copetti JB, Lorenzo E, Chenlo F. A general battery model for PV system simulation. Progress in Photovoltaics: Research and Applications 1993; 1: 283-292.

[28] Delarue E, Cattysse D, D'haeseleer W. Enhanced priority list unit commitment method for power systems with a high share of renewables. Electric Power Systems Research 2013; 105: 115-2013.

[29] Senjyu T, Miyagi T, Saber AY, Urasaki N, Funabashi T. Emerging solution of large-scale unit commitment problem by stochastic priority list. Electric Power Systems Research 2006; 76: 283-292.

[30] Dieu VN, Ongsakul W. Ramp rate constrained unit commitment by improved priority list and augmented Lagrange Hopfield network. Electric Power Systems Research 2008; 78: 291-301.

[31] Chandram K, Subrahmanyam N, Sydulu M. Unit commitment by improved pre-prepared power demand table and Muller method. International Journal of Electrical Power and Energy Systems 2011; 33: 106-114.

[32] Dieu VN, Ongsakul W. Augmented Lagrange Hopfield network based Lagrangian relaxation for unit commitment. International Journal of Electrical Power and Energy Systems 2011; 33: 522-530.

Figures Captions

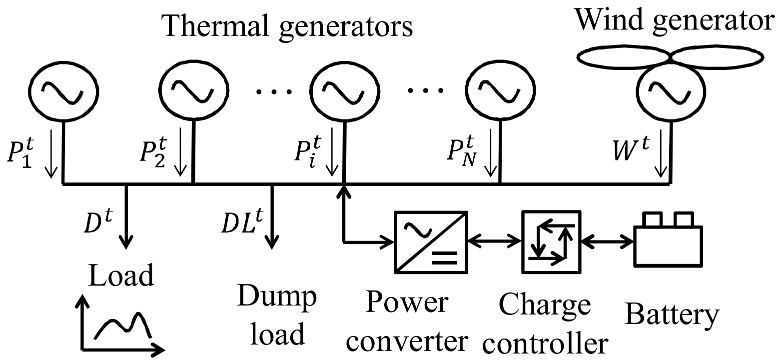

Figure 1
Architecture of the power system under analysis.

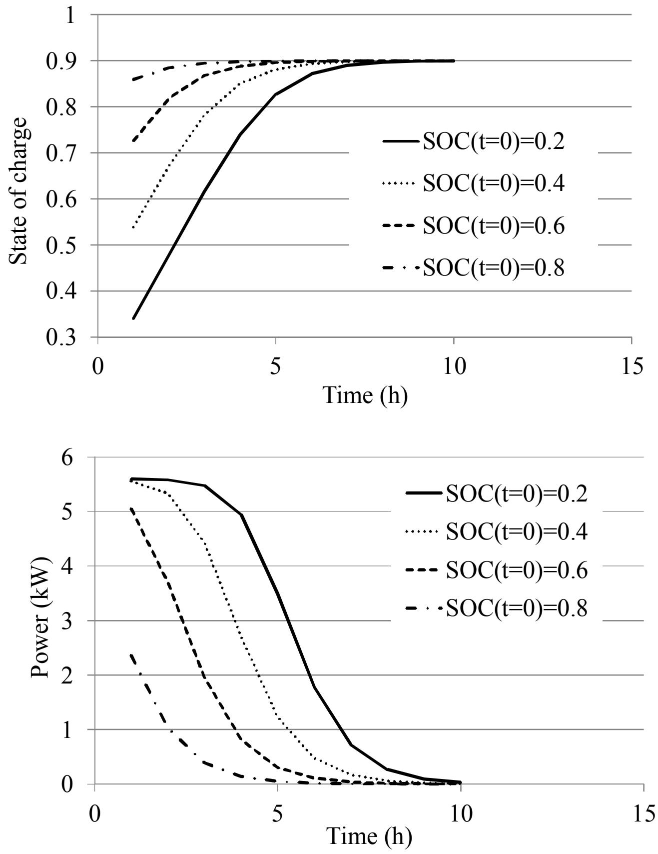

Figure 2
SOC and charging power simulation.

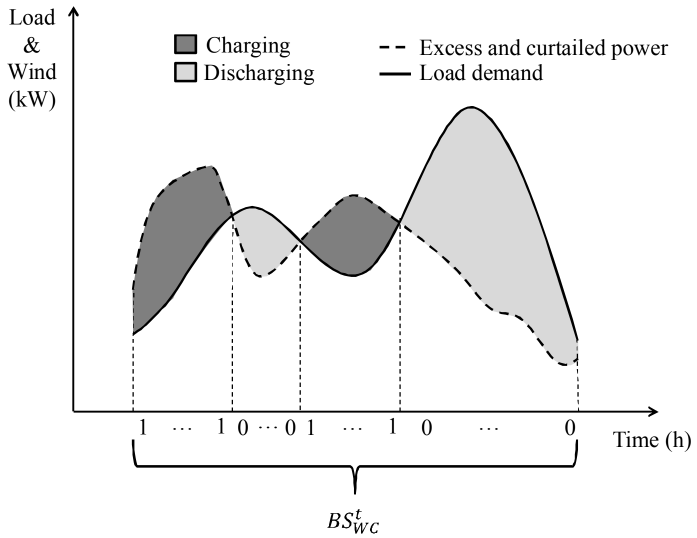

Figure 3
Charge and discharge periods according to the wind power curtailed.

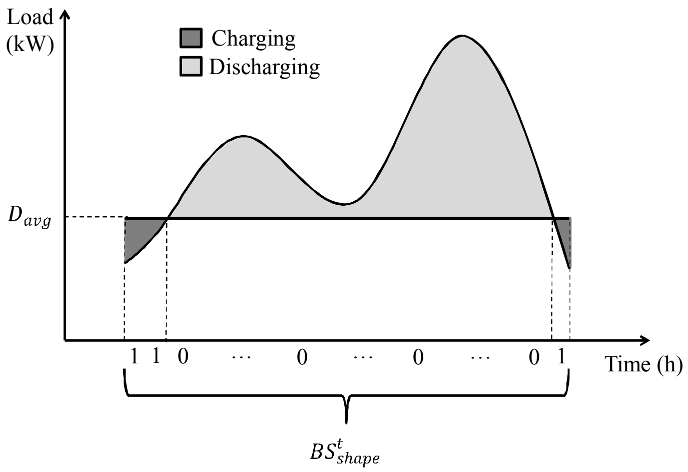

Figure 4
Charge and discharge periods according to the load profile.

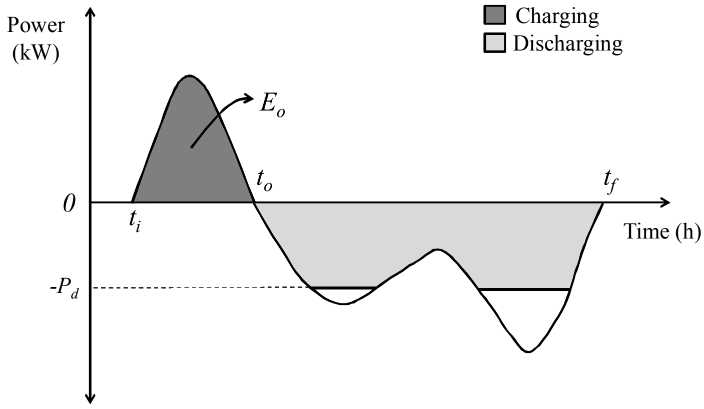

Figure 5
Reference power of BESS.

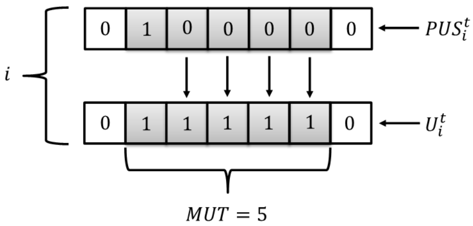

Figure 6
Repairing minimum up time constraint.

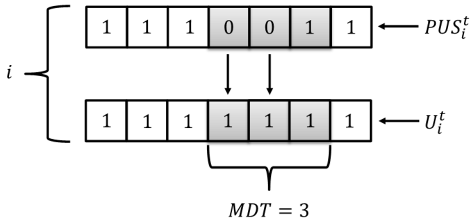

Figure 7
Repairing minimum down time constraint.

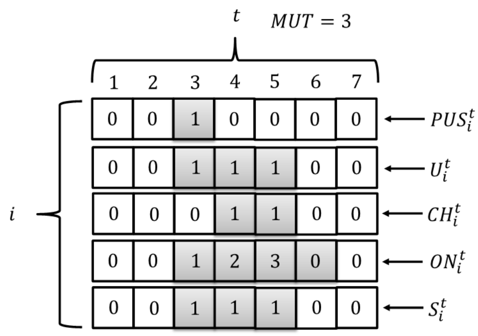

Figure 8
Selection of the units to be substituted.

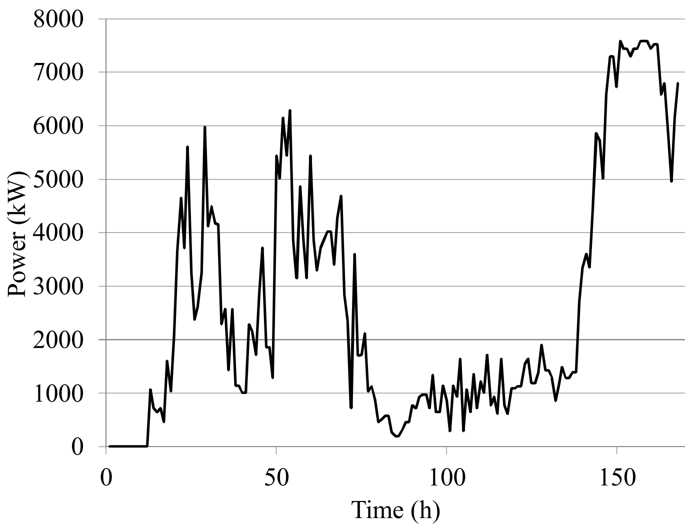

Figure 9
Hourly aggregated wind power generation.

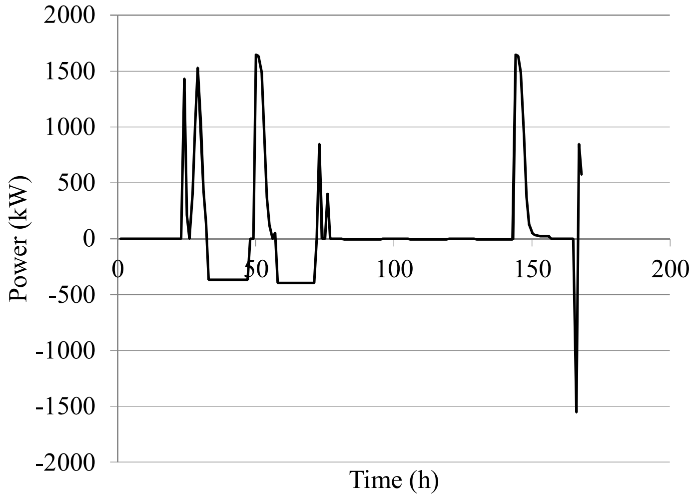

Figure 10
Power from / to BESS.

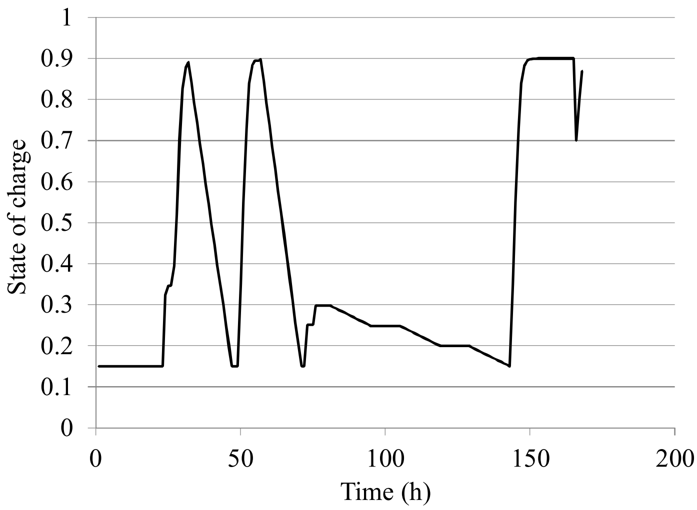

Figure 11
State-of-charge behavior.

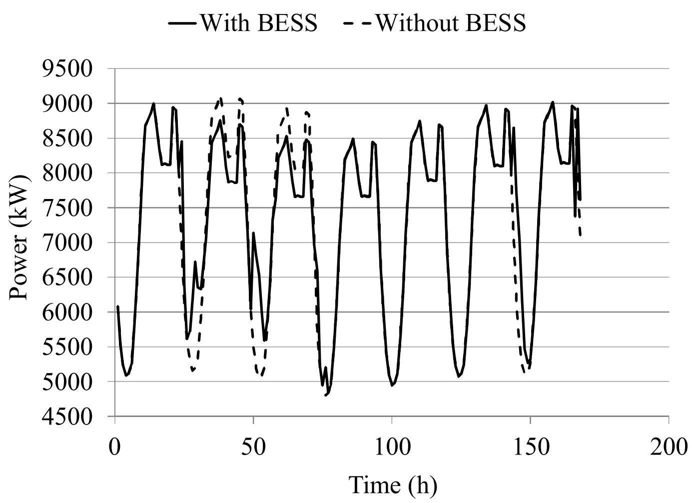

Figure 12
Load to be supplied by thermal and wind generators.

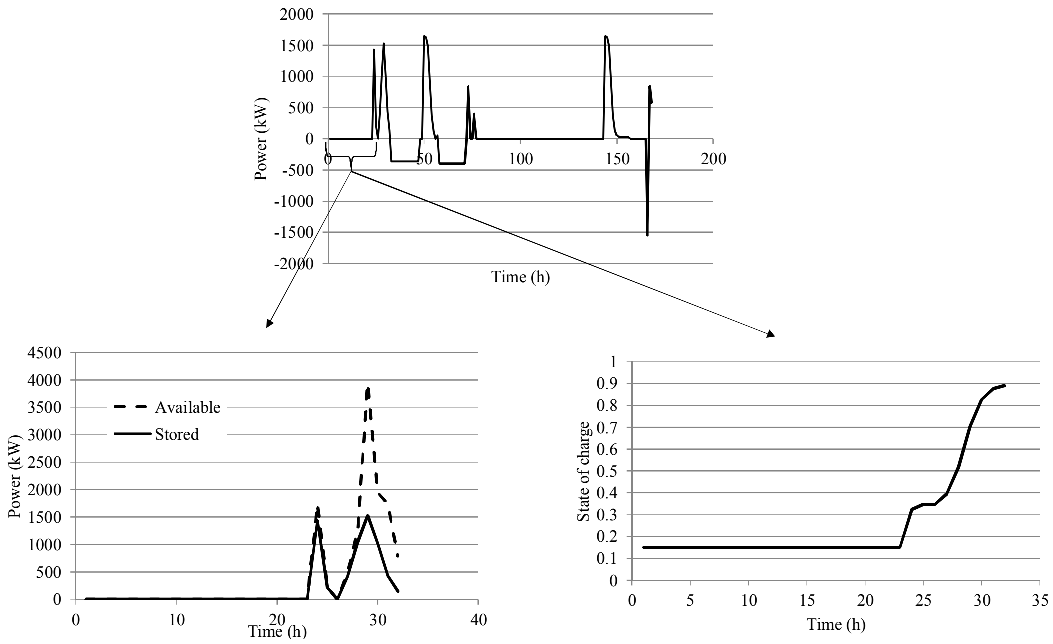

Figure 13
Performance of BESS between t=1 and t=32.

Tables Captions

Table 1
Characteristics of thermal generators.

i	P_i^{min}(kW)	P_i^{max}(kW)	a_i(L/h)	b_i(L/h)	c_i(L/kW^{2}h)
1	3150	6300	101.95	0.0868	0.000001
2	528	1056	45.2	0.1699	0.00004
3	482.5	965	13.1	0.2555	-0.000009
4	600	1200	38.8	0.1995	0.00003
5	640	1280	53.1	0.1981	0.00002

Table 2
Unit scheduling of day 2 without incorporating BESS (MW).

i	Time (h)																							
	25	26	27	28	29	30	31	32	33	34	35	36	37	38	39	40	41	42	43	44	45	46	47	48
1	3.15	3.24	3.15	3.15	3.15	3.15	3.15	3.15	3.28	5.39	5.21	5.85	5.41	6.30	6.08	5.84	6.22	5.43	5.55	5.50	5.20	4.78	5.30	5.26
2	0	0	0	0	0	0	0	0	0	0.53	0.53	0.53	0.53	0.60	0.53	0.53	0.53	0.53	0.53	0.53	0.53	0.53	0.53	0
3	0	0	0	0	0	0	0	0	0	0	**0.48**	0.48	**0.48**	0.48	0.48	0.48	0.48	0	0	**0.48**	**0.48**	0	**0.48**	0
4	0	0	0	0	0	0	0	0	0	0	0	**0.60**	0	0.60	0.60	**0.60**	0	0	0	0	0	0	0	0
5	0	0	0	0	0	0	0	0	0	0	0	0	0	0	0	0	0	0	0	0	0	0	0	0
W^t	3.02	2.38	2.16	2.00	2.04	2.18	2.75	3.40	4.15	2.29	2.58	1.43	2.58	1.14	1.14	1.00	1.00	2.29	2.15	1.72	2.86	3.72	1.86	1.86

Table 3
Unit scheduling of day 2 incorporating BESS (MW).

i	Time (h)																							
	25	26	27	28	29	30	31	32	33	34	35	36	37	38	39	40	41	42	43	44	45	46	47	48
1	3.15	3.24	3.15	3.15	3.15	3.15	3.15	3.15	3.15	5.03	5.33	6.09	5.52	6.00	5.72	6.08	5.85	5.06	5.19	5.62	5.31	4.42	5.42	5.26
2	0	0	0	0	0	0	0	0	0	0.53	0.53	0.53	0.53	0.53	0.53	0.53	0.53	0.53	0.53	0.53	0.53	0.53	0.53	0
3	0	0	0	0	0	0	0	0	0	0	**0**	0.48	**0**	0.48	0.48	0.48	0.48	0	0	**0**	**0**	0	**0**	0
4	0	0	0	0	0	0	0	0	0	0	0	**0**	0	0.60	0.60	**0**	0	0	0	0	0	0	0	0
5	0	0	0	0	0	0	0	0	0	0	0	0	0	0	0	0	0	0	0	0	0	0	0	0
W^t	3.23	2.38	2.57	3.04	3.57	3.20	3.18	3.54	3.91	2.29	2.58	1.43	2.58	1.14	1.14	1.00	1.00	2.29	2.15	1.72	2.86	3.72	1.86	1.86